INSTITUTE OF PHYSICS PUBLISHING JOURNAL OF PHYSICS A: MATHEMATICAL AND GENERAL

J. Phys. A: Math. Gen. **39** (2006) 4811–4828 doi:10.1088/0305-4470/39/18/003

Folding of polymer chains with short-range binormal interactions

A Craig and E M Terentjev

Cavendish Laboratory, Madingley Road, Cambridge CB3 0HE, UK

Received 23 January 2006
Published 19 April 2006
Online at stacks.iop.org/JPhysA/39/4811

Abstract

We study the structure of chains which have anisotropic short-range contact interactions that depend on the alignment of the binormal vectors of chain segments. This represents a crude model of hydrogen bonding or 'stacking' interactions out of the plane of curvature. The polymers are treated as ribbon-like semi-flexible chains, where the plane of the ribbon is determined by the local binormal. We show that with dipole–dipole interactions between the binormals of contacting chain segments, mean-field theory predicts a first-order transition to a binormally aligned state. We describe the onset of this transition as a function of the temperature-dependent parameters that govern the chain stiffness and the strength of the binormal interaction, as well as the binormal alignment's coupling to chain collapse. We also examine a metastable state governing the folding kinetics. Finally, we discuss the possible mesoscopic structure of the aligned phase, and application of our model to secondary structure motifs like β-sheets and α-helices, as well as composite structures like β-(amyloid) fibrils.

PACS numbers: 82.35.Jk, 87.15.−v, 87.15.Nn

1. Introduction

The 'mesoscopic' Hamiltonian has been a staple of polymer physics for the better part of a century, neglecting the chemical details of polymers in order to predict their behaviour entirely from simple geometric and energetic concerns. There exist a number of successful treatments of polymer solutions based on mesoscopic Hamiltonians, both for 'phantom' chains without excluded volume and for polymers with very simple inter-chain interactions; nematic [1–5], mixed [6, 7] or diblock polymer melts, and collapsing homopolymer [8–10] systems have each been modelled by mean-field theories or low-order loop corrections to the mean field. While the abstraction from chemistry that these mesoscopic models involve has been enormously useful, physicists have been restricted to a limited number of analytical approaches, primarily simple Edwards contact potentials that apply equally to all chain contacts, or, in the case

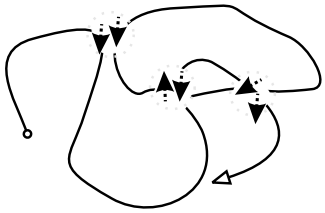

Figure 1. Worm-like chain with binormal vectors shown at the points of contact along the chain (grey circles). For $\lambda < 0$, the binormal interaction term of equation (17) favours aligned binormals like that at the left, while penalizing opposing binormals as at the centre, and neglecting nearly perpendicular binormals as at the far right.

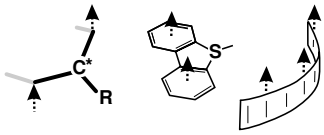

Figure 2. Schematic diagrams of chains with directional interactions, represented by dotted arrows, that are perpendicular to the plane of curvature. From the left, a single peptide residue. The dashed black bonding arrows point along the O $\rightarrow$ H direction of the hydrogen bond. In the centre, a bit of poly-benzothiophene chain, which has π-stacking interactions between aromatic groups. On the right—the abstracted chain we deal with in this paper. Here, bonding can occur at any point along the chain rather than at specific sites.

of nematic systems, an Edwards potential weighted by the chains' alignment. This neglects the highly directional nature of most chemical bonds and residue interactions. Admittedly, Lennard–Jones potentials and other, more realistic inter-chain forces feature prominently in Monte Carlo and molecular dynamics treatments. However, the simplicity and transparency of analytic methods makes the prospect of incorporating realistic, directional interactions into analytic models an appealing one.

We hope to further this goal by introducing an analytic model of single-stranded polymer chains with hydrogen-bond-like interactions. In particular, we introduce anisotropic contact interactions whose energy depends upon the orientation of the binormal vectors of intersecting chain segments, represented graphically in figure 1.

This interaction between binormals models the behaviour of chains whose backbones are decorated with dipoles that point in the direction of the chain binormal, perpendicular to the local plane of curvature as seen in the chains shown in figure 2. We intend this to serve as a crude representation of hydrogen bonds or other short-range, highly directional, 'stacking' interactions, like those between aromatic rings. These interactions are important to the behaviour of peptides and other single-stranded biopolymers, as well as artificial helicogenic polymers. Indeed, we can see that ordered structures such as α-helices and β-sheets correspond to polymers with aligned binormals, as figure 3 illustrates in the case of the α-helix. In fact, we go on to argue that the ground state of a single binormally aligning chain with excluded volume should be just such a helix.

We begin by reviewing the classical semi-flexible chain model used to describe wormlike, non-interacting polymers. However, we will at once see that in order to treat binormal interactions, we must incorporate higher-order derivatives along the chain length than those of the semi-flexible model. We therefore consider a 'bare' chain Hamiltonian in section 2,

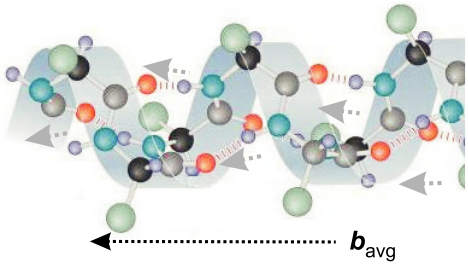

Figure 3. Diagram of α-helix, with hydrogen bonds indicated by spaced parallel lines. The grey dotted arrows denote the direction of the local binormal vector, while $\boldsymbol{b}_{\text{avg}}$ marks the average binormal produced by summing the local binormals along the entire helix length.

with a new compression-volume parameter v_p which regulates these higher-order terms. We proceed to find values of v_p that reproduce the classical semi-flexible chain statistics for a given persistence length l_p, thus fixing v_p and making contact with traditional polymer theories. With this formalism in place, one can examine the interaction between binormal vectors, which we define in the context of the 'Frenet–Serret' frame and its associated vector triplet. We incorporate interactions between binormals through a modified contact potential, then define a binormal alignment order parameter ψ corresponding to $\boldsymbol{b}_{\text{avg}}$ in figure 3, and expand the free energy in powers of $|\psi|$.

This expansion indicates that there is a first-order transition to a binormally aligned state as one increases the interaction strength $|\lambda|$, as could be induced experimentally by changes in temperature, solvent quality or ion concentration. Following the analogy with hydrogen bonding, we go on to speculate about the structure of the binormally aligned phase and its connection to helical or sheet motifs. We also observe that a collapse to a globule or a high chain concentration is necessary for a binormally ordered phase to emerge. Thus, our proposed binormal phase transition should occur as part of a sequence: coil-to-globule, then globule-to-ordered globule. This is clearly analogous to protein folding, which hierarchical models describe as starting with a collapse to a globular 'liquid droplet' followed by a local ordering into secondary structure motifs. Protein folding finishes with a tertiary-structure-forming phase we do not treat, but the resemblance to our model's sequence of phase transitions is significant. Ultimately, we assert that the model generates secondary structure motifs like β-(amyloid)-sheets, β-fibrils and α-helical structures from the generic polymer interaction we introduce.

2. Modified semi-flexible chain

Let us review the classical theory of a semi-flexible polymer chain, whose configuration is defined by the curve $\boldsymbol{r}_s$, with $\boldsymbol{r}$ being the spatial position of the monomer at a contour length s along the chain. In order to make this a model of polymers like actin or DNA which are not freely jointed, the energy of a configuration must depend on the chain's curvature. Indeed, this is the defining feature of the semi-flexible (or 'worm-like') chain model [11], for though a number of specific forms [12] have been proposed for the Hamiltonian of a semi-flexible chain, all incorporate a quadratic bending energy of the form

$$E_{\text{bend}} = \int_0^L \mathrm{d}s\, \frac{\epsilon}{2}[\kappa(s)]^2. \tag{1}$$

Here κ is the curvature defined as $\kappa = \boldsymbol{u}_s'/|\boldsymbol{u}_s|$, where $\boldsymbol{u}_s = \mathrm{d}\boldsymbol{r}_s/\mathrm{d}s$ is the tangent vector of the backbone, and the prime denotes the gradient along s, e.g. ($\boldsymbol{u}_s' = \mathrm{d}\boldsymbol{u}_s/\mathrm{d}s$).

Semi-flexible theories usually proceed by parameterizing the chain by its tangent vector $\boldsymbol{u}_s$ rather than segment position $\boldsymbol{r}_s$, and establishing the constraint $|\boldsymbol{u}_s| = 1$. This constraint can be satisfied exactly at all points on the chain, as in the Kratky–Porod chain [13], or through an average length constraint $\int_0^L \mathrm{d}s\,(\boldsymbol{u}_s)^2 = L$. Insofar as this average-length treatment is more analytically tractable than the Kratky–Porod model, in this paper we will adopt the average-constraint model and its associated Hamiltonian [14, 15]:

$$\beta\mathcal{H}[\boldsymbol{u}_s] = \int_0^L \mathrm{d}s \left[\frac{l_p}{2}\left(\frac{\mathrm{d}\boldsymbol{u}_s}{\mathrm{d}s}\right)^2 + \phi\left(\boldsymbol{u}_s^2 - 1\right)\right], \tag{2}$$

where β is the inverse temperature $(kT)^{-1}$ and l_p is the persistence length ($=\epsilon/kT$ from equation (1)) over which the chain 'remembers' its direction. The mean value of the auxiliary field ϕ acts as a Lagrange multiplier to keep the constraint of average unit tangent length.

Let us now consider a slightly altered version of the chain Hamiltonian presented in equation (2), one which includes a higher-order gradient term of the form $\frac{1}{4}v_p(\mathrm{d}^2\boldsymbol{u}_s/\mathrm{d}s^2)$, where v_p is a parameter we will refer to as the *compression volume*. Physically, this volume represents a scale over which *changes* in the rate or direction of the chain's curvature contribute to the energy. At the moment the addition of this term seems unnecessary and potentially complicating; the analogous 'jerk' terms like $\dddot{v}(t)$ in classical mechanics bring one into the regime of non-integrable dynamics [16]. Nevertheless, a higher-order gradient term will prove to be necessary to deal with the interactions introduced later in section 3. Higher-order gradients of some sort are also required to account for chiral effects like torsion, $\tau \propto \boldsymbol{u}_s \cdot (\boldsymbol{u}_s' \times \boldsymbol{u}_s'')$ [17, 18]. As such, we will persist in treating this term on the provisional assumption that its presence is justified, as we will discuss in later sections. With the higher-order change-of-curvature gradient term in place, the semi-flexible Hamiltonian of equation (2) becomes

$$\beta\mathcal{H}[\boldsymbol{u}_s] = \int_0^L \mathrm{d}s \left[\frac{v_p}{4}\left(\frac{\mathrm{d}^2\boldsymbol{u}_s}{\mathrm{d}s^2}\right)^2 + \frac{l_p}{2}\left(\frac{\mathrm{d}\boldsymbol{u}_s}{\mathrm{d}s}\right)^2 + \phi\left(\boldsymbol{u}_s^2 - 1\right)\right]. \tag{3}$$

This new Hamiltonian can be evaluated in terms of the Fourier components $\boldsymbol{u}_n$ of the tangent vector, where we have $\boldsymbol{u}_s = \sum_{n=-\infty}^{\infty} \boldsymbol{u}_n\, \mathrm{e}^{2\mathrm{i}\pi n/L}$. Note that this Fourier decomposition amounts to a choice of periodic boundary conditions in the tangent vector $\boldsymbol{u}_s$, a negligible effect in the limit of large L. We so arrive at the Fourier-space version of the Hamiltonian (3), which is a quadratic form over the set of $\boldsymbol{u}_n$,

$$\beta\mathcal{H}[\boldsymbol{u}_n] = -\phi L + \sum_{n=-\infty}^{\infty}\left(\frac{v_p}{4}\left(\frac{2\pi n}{L}\right)^4 + \frac{l_p}{2}\left(\frac{2\pi n}{L}\right)^2 + \phi\right)\boldsymbol{u}_n\boldsymbol{u}_{-n}.$$

Taking the Gaussian integral over each of the possible $\boldsymbol{u}_n$ in the partition function $Z = \int \mathcal{D}[\boldsymbol{u}_n]\,\mathrm{d}\phi\, \exp(-\beta H)$, and so deriving the free energy $\beta\mathcal{F} = -\ln Z$, we obtain

$$\beta\mathcal{F} = -\phi L + \frac{1}{2}\ln\left[\det\left(\frac{v_p}{4}\left(\frac{2\pi n}{L}\right)^4 + \frac{l_p}{2}\left(\frac{2\pi n}{L}\right)^2 + \phi\right)\right]. \tag{4}$$

We now use the identity $\ln(\det[\boldsymbol{M}]) = \mathrm{tr}(\ln[\boldsymbol{M}])$, where $\boldsymbol{M}$ is an arbitrary matrix, to evaluate the determinant as below,

$$\beta\mathcal{F} = -\phi L + \frac{3}{2}\int_{-\infty}^{\infty}\frac{L}{2\pi}\,\mathrm{d}q\,\ln\left(\frac{v_p}{4}q^4 + \frac{l_p}{2}q^2 + \phi\right), \tag{5}$$

where we have substituted integration over the continuous variable q for the summation over the discrete values of $(2\pi n/L)$ in the trace, and assumed the 3D space. Applying the saddle-point approximation for the Lagrange multiplier ϕ, namely $\partial\mathcal{F}/\partial\phi = 0$, we see

$$-L + \frac{3}{2}\int_{-\infty}^{\infty} \frac{L}{2\pi}\,\mathrm{d}q\,\frac{1}{\frac{1}{4}v_p q^4 + \frac{1}{2}l_p q^2 + \phi} = 0. \tag{6}$$

Evaluating the integral and dividing out by L, we find after a small rearrangement

$$\sqrt{\frac{1}{2}l_p + \sqrt{\frac{1}{4}l_p^2 - v_p\phi}} - \sqrt{\frac{1}{2}l_p - \sqrt{\frac{1}{4}l_p^2 - v_p\phi}} = \frac{8\sqrt{2}}{3}\phi^{1/2}\left(\frac{1}{4}l_p^2 - v_p\phi\right)^{1/2}. \tag{7}$$

Simplifying, one discovers that finding the optimal ϕ amounts to solving the cubic equation

$$\left(-81 + 144\phi l_p - 64 l_p^2\phi^2 + 256 v_p\phi^3\right) = 0. \tag{8}$$

The exact roots of this equation are rather complicated, and we simply denote the optimal energy-minimizing value of ϕ as $\phi_1(v_p, l_p)$; the other two roots of the cubic equation can be shown to be unphysical for the regime of $v_p \sim O(1)l_p^3$ we will now discuss. The complex form of equation (8) and its solutions stands in contrast to the simple result for the Lagrange multiplier, $\phi = 8/(9l_p)$, that one obtains for the semi-flexible chain governed by the Hamiltonian of equation (2) [14, 15].

We now can evaluate the tangent–tangent propagator

$$\langle \boldsymbol{u}_s \cdot \boldsymbol{u}_{s'}\rangle = \int_{-\infty}^{\infty} \frac{L}{2\pi}\,\mathrm{d}q\,\frac{\mathrm{e}^{\mathrm{i}q(s-s')}}{\frac{1}{4}v_p q^4 + \frac{1}{2}l_p q^2 + \phi_1} \tag{9}$$

which is another complicated form, obtained after the integration:

$$\begin{aligned}\langle \boldsymbol{u}_s \cdot \boldsymbol{u}_{s'}\rangle = {} & \left(\frac{1}{\frac{1}{2}l_p\mu_+ + \frac{1}{2}v_p\mu_+^3} + \frac{1}{\frac{1}{2}l_p\mu_- + \frac{1}{2}v_p\mu_-^3}\right)^{-1} \\ & \times\left(\frac{\mathrm{e}^{-\mu_+|s-s'|}}{\frac{1}{2}l_p\mu_+ + \frac{1}{2}v_p\mu_+^3} + \frac{\mathrm{e}^{-\mu_-|s-s'|}}{\frac{1}{2}l_p\mu_- + \frac{1}{2}v_p\mu_-^3}\right),\end{aligned} \tag{10}$$

where the shorthand parameters $\mu_\pm$ are the positive roots of a quadratic $v_p\mu^4/4 + l_p\mu^2/2 + \phi_1 = 0$, that is

$$\mu_\pm^2 = \frac{1}{v_p}\left(l_p \pm \sqrt{l_p^2 - 4\phi_1 v_p}\right). \tag{11}$$

For an arbitrary v_p, equation (10) indicates a multi-exponential decay of correlations in the tangent direction with chain length s, as one might expect for a chain that has two length scales in l_p and v_p/l_p^2. This stands in contrast to the single-exponential tangent–tangent correlator of the classic semi-flexible chain, which Ha and Thirumalai [14, 15] found to be

$$\langle \boldsymbol{u}_s \cdot \boldsymbol{u}_{s'}\rangle = \mathrm{e}^{-3(2l_p)^{-1}|s-s'|} \tag{12}$$

for the Hamiltonian of equation (2). However, we can recover this classical single-exponential behaviour when $\mu_+ = \mu_-$, which occurs for $v_p^* = 4l_p^3/9$. In the absence of experimental data to suggest a multi-exponential tangential correlator for a chain, we clearly wish to emphasize this case. In fact, applying v_p^* and the solution $\phi_1(v_p^*, l_p)$ to equation (10), we recover the *exact* form of the semi-flexible chain propagator of equation (12). Since the physically relevant quantities $\langle S^2\rangle$ and $\langle R^2(s-s')\rangle$ all follow from this tangential propagator, the modified chain of equation (3) will therefore fully resemble a classical semi-flexible chain if one fixes v_p at v_p^*. In this way, the formal modifications to the chain Hamiltonian made in equation (3)

can remain 'invisible' and experimentally unobservable (but still fulfilling their crucial role in making the system integrable). We therefore feel justified in applying the theory of binormal interactions that we will present in the next section to what otherwise appear to be classic, semi-flexible chains in experiments.

3. Binormal interactions

Having developed the formalism of a modified semi-flexible chain, let us now examine the binormally interacting case. This will not prove trivial, as the theory of semi-flexible polymers has not yet been as successful as earlier flexible models in describing polymers with excluded volume and other contact interactions. In dealing with fully flexible chains, polymer physics has made much use of the Edwards contact potential $E_{\text{contact}} = \nu\delta[\boldsymbol{r}_s - \boldsymbol{r}_{s'}]$ where ν is a constant [8] related to the second virial coefficient of chain self-interaction. However, this pair potential has only been applied to semi-flexible chains by approximate, perturbative techniques [19, 20] and without the deep connections to the ϕ^4 renormalization group established for fully flexible chains [21–23]. Nevertheless, Edwards and Gupta [2, 3] successfully introduced a mean-field theory of nematic semi-flexible chains with short-range (contact) interactions that tend to align the chains tangential vectors, $E_{\text{contact}} \propto -(\boldsymbol{u}_s \cdot \boldsymbol{u}_{s'})^2\delta[\boldsymbol{r}_s - \boldsymbol{r}_{s'}]$. This model has seen wide applications in liquid crystal systems and even been incorporated into analytic treatments of protein-like rod-coil systems [24, 25]. We propose an extension of these methods to account for anisotropic interactions between polymers, motivated by both Monte Carlo studies of helix-forming chains that suggest anisotropic interactions are key to peptide secondary structures [26], and a desire to approximate the effects of hydrogen bonding in peptide α-helices and artificial helical polymers, where the direction of bonding is perpendicular to the chain's plane of curvature. To do so, we will consider interactions between the binormal vectors of a chain, which we define below.

Let us return to the case of a polymer with a backbone trajectory that follows the continuous, differentiable space curve $\boldsymbol{r}_s$. Given $\boldsymbol{r}_s$, we can define a Frenet–Serret frame of three orthogonal vectors [17] that rest on the curve: the unit tangent vector $\hat{\boldsymbol{u}}_s$, the unit normal vector $\hat{\boldsymbol{n}}_s$, and the unit binormal vector, $\hat{\boldsymbol{b}}_s$, which are given by the relations

$$\hat{\boldsymbol{u}}_s = \frac{\boldsymbol{r}'_s}{|\boldsymbol{r}'_s|}, \qquad \hat{\boldsymbol{n}}_s = \frac{\hat{\boldsymbol{u}}'_s}{|\hat{\boldsymbol{u}}'_s|}, \qquad \hat{\boldsymbol{b}}_s = \hat{\boldsymbol{u}}_s \times \hat{\boldsymbol{n}}_s, \tag{13}$$

where the 'hat' symbol marks vectors normalized to unit length.

The derivatives of the unit frame vectors with respect to s, which we again denote by the prime symbol, e.g. $\boldsymbol{r}'_s = \mathrm{d}\boldsymbol{r}/\mathrm{d}s$, are linked to the original frame vectors by the Frenet–Serret formula(s)

$$\hat{\mathbf{u}}'_s = \kappa(s)\hat{\boldsymbol{n}}_s \tag{14}$$

$$\hat{\mathbf{n}}'_s = -\kappa(s)\hat{\boldsymbol{u}}_s + \tau(s)\hat{\boldsymbol{b}}_s \tag{15}$$

$$\hat{\mathbf{b}}'_s = -\tau(s)\hat{\mathbf{n}}_s, \tag{16}$$

where $\kappa(s)$ is the curvature and $\tau(s) = (\boldsymbol{u}_s \cdot [\boldsymbol{u}'_s \times \boldsymbol{u}''_s])/[\kappa(s)]^2$ is the torsion for a chain with unit tangent length.

Since it fully specifies the orientation of a chain, the Frenet–Serret frame suggests itself naturally as a tool for polymer physics and has a long history of applications [12, 18]. In physical terms, the tangent is simply the instantaneous direction of the backbone and the normal the direction of its curvature. Taken together at a given s, the tangent and normal

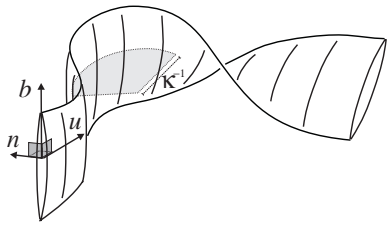

Figure 4. Directed, ribbonlike polymer with associated Frenet–Serret frame of tangent (**u**), normal (**n**) and binormal vectors (**b**). Following the convention that the polymer curves along its 'thin' direction, the binormal will always point along the ribbon's thicker direction. We also indicate the radius of curvature (κ^{-1}) in a region of roughly constant curvature.

vectors define the local plane of curvature of the space curve, while the binormal defines the perpendicular to that plane [17, 27]. Analogously, if one imagines a polymer chain as an oriented ribbon which can only curve along its 'thin' direction as in figure 4, the binormal defines the direction of the plane of the ribbon. This fact has been explicitly developed to model ribbon-like polymers [28–31] with separate bending moduli along the two axes of the ribbon. These models display interesting twist dynamics [31] and phase behaviour [29] as a result of their local anisotropy.

Having defined the binormal vector on a chain, we modify equation (3) to include a 'dipolar' interaction based on the binormal (rather than tangential) alignment of two crossing polymer segments.

$$\beta\mathcal{H}[\boldsymbol{u}_s, \boldsymbol{b}_s] = \int_0^L \mathrm{d}s \left[\frac{v_p}{4} \left(\frac{\mathrm{d}^2\boldsymbol{u}_s}{\mathrm{d}s^2} \right)^2 + \frac{l_p}{2} \left(\frac{\mathrm{d}\boldsymbol{u}_s}{\mathrm{d}s} \right)^2 + \phi(\boldsymbol{u}_s^2 - 1) \right] + \lambda \int_0^L \mathrm{d}s\, \mathrm{d}s'\, (\boldsymbol{b}_s \cdot \boldsymbol{b}_{s'})\, \delta[\boldsymbol{r}_s - \boldsymbol{r}_{s'}] + \nu \int_0^L \mathrm{d}s\, \mathrm{d}s'\, \delta[\boldsymbol{r}_s - \boldsymbol{r}_{s'}]. \tag{17}$$

Note that we use the full binormal $\boldsymbol{b}_s = [\boldsymbol{u}_s \times \boldsymbol{u}_s']$, and not the unit vector, $\hat{\boldsymbol{b}}_s = [\boldsymbol{u}_s \times \boldsymbol{u}_s']/(|\boldsymbol{u}_s||\boldsymbol{u}_s'|)$, in establishing the binormal interaction, whose strength and aligning/anti-aligning character are controlled by the magnitude and sign of λ, respectively. In addition to the binormal interaction, we include the term parameterized by ν as a usual Edwards contact potential that determines the energy of intersecting chain segments irrespective of their binormal alignment [8].

Though the form of equation (17) is fairly straightforward, its physical interpretation merits further discussion. First, we note that defining the (variable-length) binormal vector as $\boldsymbol{b}_s = [\boldsymbol{u}_s \times (\mathrm{d}\boldsymbol{u}_s/\mathrm{d}s)]$ and not as a free, auxiliary field as others have done [28–31] means that the chain is completely inflexible in the direction of the binormal, i.e. has infinite bending modulus for curvature in the binormal plane. However, our Hamiltonian lacks an explicit twist-energy term $\propto(\mathrm{d}\boldsymbol{b}_s/\mathrm{d}s)^2$ common to many treatments of ribbon-like polymers, so the plane of the polymer's curvature appears free to rotate in our model. The absence of a twist term is grounded in concerns about the integrability of this term for our definition of $\boldsymbol{b}_s$, and the observation that the twist rotation of many biomolecules is much shorter than their overall persistence length, e.g. dsDNA has a 3 nm pitch against its 120 nm persistence length [32]. Regardless, we will see that changes in the direction of the binormal are constrained by the change-of-curvature term in our Hamiltonian $\propto v_p$.

Indeed, the reasons for adding the change-of-curvature term to equation (17) are still not obvious. We can first justify this term's presence by noting that the binormal alignment terms

controlled by λ should contribute an energy proportional to the curvature squared. Thus, if we have a Hamiltonian that has a bending energy penalty $E_{\rm bend} = \frac{1}{2} l_p [\kappa(s)]^2$, a negative λ with $|\lambda| > l_p/2$ will result in the chain having a negative energy penalty associated with curvature. This situation mirrors a Lagrangian dynamical system with a potential energy depending on acceleration, leading to an effective negative mass [16]. We must avoid such a disaster by accounting for higher-order chain-gradient terms in our Hamiltonian, similar to the case in the work of Gupta and Edwards [2]. Taking the lowest-order such term, $\propto(\mathrm{d}^2\boldsymbol{u}_s/\mathrm{d}s^2)$ is analogous to adding a kinetic energy term with $\ddot{v}(t)$ in Lagrangian dynamics. While the inclusion of such a term might be difficult to justify in a dynamical Hamiltonian, it emerges much more plausibly in a description of the mechanical response of materials like the semi-flexible model of a polymer chain.

We also note that the $(\mathrm{d}^2\boldsymbol{u}_s/\mathrm{d}s^2)$ term recapitulates the influence of the seemingly neglected twist-energy term $\propto (\mathrm{d}\boldsymbol{b}_s/\mathrm{d}s)^2$. Indeed, the Frenet–Serret connection $\boldsymbol{b}_s' = \tau(s)\boldsymbol{n}_s$ (where $\tau(s)$ is the torsion) between the normal vector $\boldsymbol{n}_s$ and binormal vector $\boldsymbol{b}_s$ means that v_p effectively penalizes changes to $\boldsymbol{n}$ by the relation $\boldsymbol{u}_s'' = d/\mathrm{d}s([\tau(s)]^{-1}\boldsymbol{b}_s')$. Working through with the chain rule, it follows that $\frac{1}{4}v_p\,(\mathrm{d}^2\boldsymbol{u}_s/\mathrm{d}s^2)$ contributes to an effective twist-energy term.

Finally, we observe that our choice of a dipolar interaction for the binormal alignment may not be as directionally specific as real hydrogen bonds [26]. Nonetheless, the dipolar form offers the benefits of being analytically tractable and the natural first term in a multipolar expansion of any more complicated angular potential. The choice of a dipolar interaction also makes this work the natural extension of past studies of polymers with èmbedded' electric or magnetic dipoles in an external field [18]. Nonetheless, our treatment differs in that the model is based on short-range interactions between or within chains, which sets our physical situation apart from external-field models in the same way a polymer chain in a nematic melt differs from a chain aligned with an imposed external force.

The Hamiltonian of equation (17) is not yet analytically tractable, but we can simplify it by the identity

$$\int \mathrm{d}s\,\mathrm{d}s'\, f(\boldsymbol{r}_s) f(\boldsymbol{r}_s')\delta[\boldsymbol{r}_s - \boldsymbol{r}_{s'}] = \int \mathrm{d}\boldsymbol{R}\,(f(\boldsymbol{r}_s)\delta[\boldsymbol{r}_s - \boldsymbol{R}])^2, \tag{18}$$

where $f(s)$ and $f(s')$ are arbitrary functions of s and s', respectively. We can move further towards solving this system by establishing an order parameter ψ for the net binormal alignment such that $\psi \propto \int_0^L \mathrm{d}s\,[\boldsymbol{u}_s \times \boldsymbol{u}_s']$. We likewise address the Edwards contact potential by adding the 'line concentration' field, or the density $\rho(\boldsymbol{R}) = \int \mathrm{d}s\,\delta[\boldsymbol{r}_s - \boldsymbol{R}]$. These objects can be introduced to the partition function by adding two delta-functions,

$$\begin{aligned} Z = \int \mathcal{D}[\boldsymbol{u}_s] \prod_{\boldsymbol{R}} \delta\left(\rho(\boldsymbol{R}) - \int_0^L \mathrm{d}s\,\delta[\boldsymbol{r}_s - \boldsymbol{R}]\right) \\ \times \delta\left(\boldsymbol{\psi}(\boldsymbol{R}) - \int_0^L \mathrm{d}s\,\boldsymbol{b}_s\,\delta[\boldsymbol{R} - \boldsymbol{r}_s]\right) \mathrm{e}^{-\beta\mathcal{H}[\boldsymbol{u}_s, \boldsymbol{b}_s]} \end{aligned} \tag{19}$$

which we can now treat by replacing the δ-functions with their exponentiated forms,

$$\int \mathcal{D}[\tilde{\boldsymbol{\xi}}(\boldsymbol{R})] \exp\left(\int \mathrm{d}\boldsymbol{R}\,\mathrm{i}\tilde{\boldsymbol{\xi}}(\boldsymbol{R}) \cdot \left[\boldsymbol{\psi}(\boldsymbol{R}) - \int_0^L \mathrm{d}s\,\left(\boldsymbol{u}_s \times \frac{\mathrm{d}\boldsymbol{u}_s}{\mathrm{d}s}\right)\delta[\boldsymbol{R} - \boldsymbol{r}_s]\right]\right) \tag{20}$$

and

$$\int \mathcal{D}[\tilde{\omega}(\boldsymbol{R})] \exp\left(\int \mathrm{d}\boldsymbol{R}\left[\mathrm{i}\tilde{\omega}(\boldsymbol{R})(\rho(\boldsymbol{R}) - \int_0^L \mathrm{d}s\,\delta[\boldsymbol{r}_s - \boldsymbol{R}])\right]\right). \tag{21}$$

Note that we have written out $\boldsymbol{b}_s$ explicitly in equation (20). Throughout the remainder of this paper we will make the field substitutions $\boldsymbol{\xi} = \mathrm{i}\tilde{\boldsymbol{\xi}}$ and $\omega = \mathrm{i}\tilde{\omega}$, to simplify notation. The new fields $\boldsymbol{\xi}$, ψ, ω and ρ in the exponential leave us with the effective Hamiltonian

$$\begin{aligned}\beta\mathcal{H}[\boldsymbol{u}_s, \boldsymbol{\xi}(\boldsymbol{R}), \psi(\boldsymbol{R}), \rho(\boldsymbol{R}), \omega(\boldsymbol{R}))] = \int_0^L \mathrm{d}s \Bigg[\frac{v_p}{4}\left(\frac{\mathrm{d}^2\boldsymbol{u}_s}{\mathrm{d}s^2}\right)^2 \\ + \frac{l_p}{2}\left(\frac{\mathrm{d}\boldsymbol{u}_s}{\mathrm{d}s}\right)^2 + \phi\left(\boldsymbol{u}_s^2 - 1\right) - \boldsymbol{\xi}(\boldsymbol{r}_s)\cdot\left(\boldsymbol{u}_s \times \frac{\mathrm{d}\boldsymbol{u}_s}{\mathrm{d}s}\right) - \omega(\boldsymbol{r}_s)\Bigg] \\ + \int \mathrm{d}\boldsymbol{R}\,(\lambda[\psi(\boldsymbol{R})]^2 + \boldsymbol{\xi}(\boldsymbol{R})\cdot\psi(\boldsymbol{R}) + \nu[\rho(\boldsymbol{R})]^2 + \rho(\boldsymbol{R})\omega(\boldsymbol{R})) \qquad (22)\end{aligned}$$

and a partition function

$$\mathcal{Z} = \int \mathcal{D}[\boldsymbol{u}_s]\,\mathcal{D}[\boldsymbol{\xi}(\boldsymbol{R})]\,\mathcal{D}[\omega(\boldsymbol{R})]\,\mathrm{e}^{\beta\mathcal{H}[\boldsymbol{u}_s, \boldsymbol{\xi}(\boldsymbol{R}), \psi(\boldsymbol{R}), \rho(\boldsymbol{R}, \omega(\boldsymbol{R}))]}.$$

Note that for simplicity we will use $\beta\mathcal{H}[\boldsymbol{u}_s]$ to denote the Hamiltonian of equation (22) through the rest of this paper.

4. Mean field theory

The Hamiltonian of equation (22) appears formidable, but we now treat it with the mean-field approximation that $\boldsymbol{\xi}$, ψ, ρ and ω each take constant values across all of space, changing equation (22) to

$$\begin{aligned}\beta\mathcal{H}[\boldsymbol{u}_s] = V[\lambda\psi^2 + \boldsymbol{\xi}\cdot\psi + \nu\rho^2 + \omega\rho] + \int_0^L \mathrm{d}s \Bigg[v_p\left(\frac{\mathrm{d}^2\boldsymbol{u}_s}{\mathrm{d}s^2}\right)^2 \\ + \frac{l_p}{2}\left(\frac{\mathrm{d}\boldsymbol{u}_s}{\mathrm{d}s}\right)^2 + \phi(\boldsymbol{u}_s^2 - 1) - \boldsymbol{\xi}\cdot\left[\boldsymbol{u}_s \times \frac{\mathrm{d}\boldsymbol{u}_s}{\mathrm{d}s}\right] - \omega\Bigg], \qquad (23)\end{aligned}$$

where V is the volume of integration over $\boldsymbol{R}$.

The Hamiltonian of equation (23) readily yields to analysis in terms of the Fourier components used previously to evaluate equation (3). In terms of the Fourier components, we have another quadratic form

$$\begin{aligned}\beta\mathcal{H}[\boldsymbol{u}_s] = -(\phi + \omega)L + V\left[\lambda(\psi^\alpha)^2 + \xi^\alpha\psi^\alpha + \nu\rho^2 + \omega\rho\right] \\ + \sum_{n=-\infty}^{\infty}\left(\left[\frac{v_p}{4}\left(\frac{2\pi n}{L}\right)^4 + \frac{l_p}{2}\left(\frac{2\pi n}{L}\right)^2 + \phi\right]\delta_{\alpha\beta} - \xi^\gamma\epsilon_{\alpha\beta\gamma}\frac{2\mathrm{i}\pi n}{L}\right)u^\alpha_{-n}u^\beta_{n'}. \qquad (24)\end{aligned}$$

We now integrate over the Gaussian variables $\boldsymbol{u}_n$ to simplify the partition function Z for the Hamiltonian given in equation (24). Again taking $\beta\mathcal{F} = -\ln(Z)$, we see that

$$\beta\mathcal{F} = -(\phi + \omega)L + V[\lambda\psi^2 + \boldsymbol{\xi}\cdot\psi + \nu\rho^2 + \omega\rho] + \frac{1}{2}\ln\left[\det M^{\alpha\beta}_{n,n'}\right], \qquad (25)$$

where

$$M^{\alpha\beta}_{n,n'} = \left(\left[\frac{v_p}{4}\left(\frac{2\pi n}{L}\right)^4 + \frac{l_p}{2}\left(\frac{2\pi n}{L}\right)^2 + \phi\right]\delta_{\alpha\beta} - \xi^\gamma\epsilon_{\alpha\beta\gamma}\frac{2\mathrm{i}\pi n}{L}\right)\delta_{n,n'}. \qquad (26)$$

The problem is somewhat unusual because it involves an antisymmetric component of the matrix kernel of the Gaussian integral. One of the ways to treat this situation is to diagonalize this matrix in its (α, β) components. To achieve this we begin by decomposing $M^{\alpha\beta}_{n,n'}$ into

blocks of a given n, i.e. $\tilde{M}_1^{\alpha\beta} \oplus \tilde{M}_2^{\alpha\beta} \oplus \ldots$. Since $\det(A_0 \oplus A_1) = \det(A_0)\det(A_1)$, and $\det(A_k) = \prod_a \lambda_a^k$, where λ_a^k is the ath eigenvalue of A_k, we can rewrite $\det\left(M_{n,n'}^{\alpha\beta}\right)$ as $\prod_a \det(M^a)$, where M^a is the diagonal eigenvalue matrix $M_{1,1}^a \oplus M_{2,2}^a \oplus \ldots$ and a again serves as the eigenvalue index. We find the nth element $M_{n,n'}^a$ of M^a by solving for the roots of the characteristic equation $\det\left(M_{n,n'}^{\alpha\beta} - M_{n,n'}^a \mathbb{I}\right) = 0$, where $\mathbb{I}$ is the identity matrix. Proceeding through this calculation, one finds that the three eigenvalues of (3×3) matrix $M^{\alpha\beta}$ take the form

$$M_{n,n'}^a = \frac{v_p}{4}\left(\frac{2\pi n}{L}\right)^4 + \frac{l_p}{2}\left(\frac{2\pi n}{L}\right)^2 + \mathrm{i}\left(\frac{2\pi n}{L}\right)\xi_a + \phi, \tag{27}$$

where the coefficients ξ_a are given by the set

$$\{\xi_0, \xi_+, \xi_-\} = \{0, \mathrm{i}|\boldsymbol{\xi}|, -\mathrm{i}|\boldsymbol{\xi}|\}. \tag{28}$$

The imaginary nature of the ξ_a follows from the antisymmetric character of the matrix $\epsilon_{\alpha\beta\gamma}$, just as symmetric matrices necessarily produce real-value eigenvalues. Fortunately, we will see that the imaginary character of the ξ_a will have no unphysical consequences for our model.

The product $\prod_a \det(M^a)$ can now be evaluated with the help of the identity $\ln[\det(f)] = \mathrm{tr}[\ln(f)]$, followed by an integral approximation to the discrete sum over n in the trace. This approximation has the form $\mathrm{tr}_n = \int_{-\infty}^{\infty} \mathrm{d}q\, L/(2\pi)$, where $q = 2n\pi/L$ and tr_n denotes the sum over n. Thus, the free energy becomes

$$\begin{aligned}\beta\mathcal{F} = &-(\phi+\omega)L + V[\lambda\psi^2 + \boldsymbol{\xi}\cdot\boldsymbol{\psi} + \nu\rho^2 + \omega\rho] \\ &+ \frac{1}{2}\sum_{a=1}^{3}\int_{-\infty}^{\infty}\mathrm{d}q\,\frac{L}{2\pi}\ln\left(\frac{v_p}{4}q^4 + \frac{l_p}{2}q^2 + \phi - \mathrm{i}q\xi_a\right).\end{aligned} \tag{29}$$

The q-integral in equation (29) can be evaluated exactly by decomposing the quartic polynomial in q under the logarithm into the product of two quadratic forms in q,

$$\begin{aligned}\beta\mathcal{F} = &-(\phi+\omega)L + V[\lambda\psi^2 + \boldsymbol{\xi}\cdot\boldsymbol{\psi} + \nu\rho^2 + \omega\rho] + \frac{L}{4\pi}\sum_a\int_{-\infty}^{\infty}\mathrm{d}q \\ &\times\ln\left[\left(\frac{1}{2}\sqrt{v_p}q^2 + H_a q + J_a\right)\left(\frac{1}{2}\sqrt{v_p}q^2 - H_a q + \frac{\phi}{J_a}\right)\right],\end{aligned} \tag{30}$$

where the coefficients H_a and J_a are determined by the set of equations

$$\mathrm{i}J_a\xi_a = H_a\left(\phi - J_a^2\right) \tag{31}$$

$$J_a\frac{l_p}{2} = -H_a^2 J_a + \frac{1}{2}\sqrt{v_p}\left(\phi + J_a^2\right). \tag{32}$$

While these equations admit of multiple solutions for H_a and J_a, we choose to keep continuity with the classical semi-flexible chain with the Hamiltonian of equation (3) by taking the solutions which remain analytic in the limit $\xi_a \to 0, \forall a$ which reproduces the case of no binormal interactions, i.e. $\lambda = 0$. With this condition, we find J_a to be the solution

$$J_a = \frac{1}{\sqrt{v_p}}\left(\frac{l_p}{2} + H_a^2 \pm \sqrt{\left(\frac{l_p}{2} + H_a^2\right)^2 - v_p\phi}\right). \tag{33}$$

Irrespective of our choice of the sign in front of the square root in equation (33), H_a^2 emerges as the positive, real root of the bi-cubic equation

$$-\frac{1}{4}v_p\xi_a^2 + \left(\frac{l_p^2}{4} - v_p\phi\right)H_a^2 + l_p H_a^4 + H_a^6 = 0 \tag{34}$$

which for $\{\phi, \frac{1}{2}l_p\} > 0$ happens to be given by

$$H_a^2 = \frac{1}{6\chi_a}\left(2^{-\frac{2}{3}}l_p^2 + 3(2^{\frac{4}{3}})v_p\phi - 2l_p\chi_a + 2^{\frac{2}{3}}\chi_a^2\right), \tag{35}$$

where the shorthand parameter χ_a stands for

$$\chi_a^3 = \frac{l_p^3}{4} - \frac{27}{4}v_p\xi_a^2 - 9v_pl_p\phi + \sqrt{-4\left(\frac{l_p^2}{4} + 3v_p\phi\right)^3 + 2\left(\frac{l_p^3}{4} - \frac{27}{4}v_p\xi_a^2 - 9v_pl_p\phi\right)^2}. \tag{36}$$

Note that ξ_a always appears as a square in these solutions, indicating that we need not be concerned by the fact that the eigenvalues were imaginary. With equation (35) for H_a, we now have a logarithm of the product of two quadratic functions in q, which we then split into the sum of the quadratic logarithms. The integral over such a quadratic logarithm can be evaluated by the relation

$$\int_{-\infty}^{\infty}\frac{\mathrm{d}q}{2\pi}\left[\ln(a_2q^2 + a_1q + a_0)\right] \Rightarrow \frac{\sqrt{-a_1^2 + 4a_2a_0}}{4a_2}, \tag{37}$$

where the a_k are constants, and $\Rightarrow$ indicates that we have dropped infinite terms $\propto q|_{-\infty}^{\infty}$ so as to deal only with the finite part of the excess free energy that depends upon the parameters of our model. In this way, equation (30) becomes

$$\beta\mathcal{F} = -(\phi + \omega)L + V[\lambda\psi^2 + \boldsymbol{\xi}\cdot\boldsymbol{\psi} + \rho\omega + \nu\rho^2] + \frac{L}{2\sqrt{v_p}}\sum_a\left(\sqrt{2\sqrt{v_p}J_a - H_a^2} + \sqrt{2\sqrt{v_p}\frac{\phi}{J_a} - H_a^2}\right). \tag{38}$$

The undetermined Lagrange multiplier ϕ and auxiliary fields $\boldsymbol{\xi}$ and ω can now be fixed by taking saddle-point approximations for these variational parameters, which require $\partial\mathcal{F}/\partial\phi = 0$ and $\delta\mathcal{F}/\delta\boldsymbol{\xi} = 0$, $\delta\mathcal{F}/\delta\boldsymbol{\omega} = 0$. One can see that the equation $\delta\mathcal{F}/\delta\boldsymbol{\omega} = 0$ yields a simple result,

$$-L + V\rho = 0. \tag{39}$$

This fixes the average value for ρ and produces several constant terms in (38), in addition to the term $V\lambda\psi^2$ that will contribute to the final free energy expansion in powers of this order parameter.

Unfortunately, the complicated dependence of H_a and J_a on the two remaining mean fields, ϕ and $\boldsymbol{\xi}$, means we do not have an obvious analytic solution for the system of equations that result from their saddle-point conditions. Nevertheless, we can hope to arrive at approximate values for ϕ and $\boldsymbol{\xi}$ simply by following some qualitative characteristics of the free energy. As a function in the plane of possible $\{\phi, |\boldsymbol{\xi}|\}$ values, the free energy of equation (38) can be thought of as being made of two parts, a linear 'background'

$$\mathcal{F}_{\text{back}} = -\phi L + V\boldsymbol{\xi}\cdot\boldsymbol{\psi} \tag{40}$$

and the square-root dependent 'body'

$$\mathcal{F}_{\text{body}} = \frac{L}{2\sqrt{v_p}}\sum_a\left(\sqrt{2\sqrt{v_p}J_a - H_a^2} + \sqrt{2\sqrt{v_p}\frac{\phi}{J_a} - H_a^2}\right). \tag{41}$$

We know a saddle point will occur where the gradients of the energies $\mathcal{F}_{\text{back}}$ and $\mathcal{F}_{\text{body}}$ cancel, that is, they have equal magnitudes and point in opposite directions in the $\{\phi, |\boldsymbol{\xi}|\}$ plane. Finding the exact point at which this occurs is a matter of solving the system of equations $\partial\mathcal{F}/\partial\phi = 0$ and $\partial\mathcal{F}/\partial\boldsymbol{\xi} = 0$, which is not analytically practical, but we can find the *general location* of the solution by a rough heuristic argument. First, we observe that $\mathcal{F}_{\text{body}}$ changes

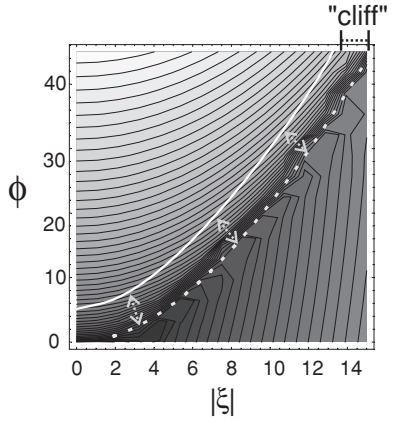

Figure 5. Contour plot of the body free energy of equation (41) plotted in the (ξ, ϕ) plane. The dashed line marks the boundary below which the free energy ceases to be real-valued, while the solid white line marks the rough boundary of the 'cliff' region of rapid change over which the gradient is steepest.

most rapidly along the 'cliff' shown in figure 5 that rises near the line where $\sqrt{2\sqrt{v_p}J_a - H_a^2}$ becomes complex for the ξ-dependent eigenvalues of $a = \pm$. If $\mathcal{F}_{\text{back}}$ is steep enough, we can be confident that the saddle point lies near the cliff, since we need the gradients of $\mathcal{F}_{\text{body}}$ and $\mathcal{F}_{\text{back}}$ to cancel. The cliff's edge is defined by the equation $\text{Im}[\chi_\pm] = 0$, or

$$4\left(\frac{l_p^2}{4} + 3v_p\phi\right)^3 = \left(\frac{l_p^3}{4} + \frac{27}{4}v_p|\boldsymbol{\xi}|^2 - 9v_p l_p\phi\right)^2. \tag{42}$$

We can check that the solution should lie near the cliff by performing a numerical expansion of the free energy of equation (41) along the ϕ direction such that $\phi = \phi_{\text{cliff}} + \Delta\phi$, where ϕ_{cliff} is the value of ϕ set for a given $|\boldsymbol{\xi}|$ in equation (42). For the semi-flexible-like case where $v_p = v_p^*$ we find that at $\Delta\phi = l_p^{-1}$, $\partial_\phi\mathcal{F}_{\text{body}} \approx L$ for all $|\boldsymbol{\xi}|$. This is the condition for $\partial_\phi\mathcal{F}_{\text{body}}$ to cancel $\partial_\phi\mathcal{F}_{\text{back}}$, which is $-L$ everywhere. As well, we find that $\partial_\phi^2\mathcal{F}_{\text{body}} \approx -l_p L$ at $\Delta\phi \approx l_p^{-1}$, indicating that the approximate location for the saddle point is well localized around $\Delta\phi = l_p^{-1}$. Thus, the solution will lie near the cliff edge for any appreciable persistence length l_p.

We have now approximated the distance $\Delta\phi$ away from the cliff edge where we will find our solution, but $|\boldsymbol{\xi}|$ remains unfixed. We could calculate the distance $\Delta|\boldsymbol{\xi}|$ from the cliff's edge where the magnitudes of the derivatives $\partial_{|\boldsymbol{\xi}|}\mathcal{F}_{\text{body}}$ and $\partial_{|\boldsymbol{\xi}|}\mathcal{F}_{\text{back}}$ cancel, as we did with ϕ. However, this would not tell us where the *directions* of the gradients cancel, just that they do so near the cliff. We will therefore take a more general approach.

We still assume that the solution lies near the cliff in $\mathcal{F}_{\text{body}}$, since the magnitude of $\nabla\mathcal{F}_{\text{body}}$ adopts values from infinity to nearly zero in this region, much as the gradient of $\sqrt{x}$ does for $x = O(1)$. As such, we avoid calculating the magnitude of the gradient of $\mathcal{F}_{\text{body}}$, since we assume it adopts the appropriate value to cancel $\nabla\mathcal{F}_{\text{back}}$ somewhere near the cliff. Since $\nabla\mathcal{F}_{\text{body}}$ points nearly perpendicular to the cliff edge for some distance from the cliff edge, as illustrated by figure 5, we will assume the gradient's direction is constant in this vicinity. Thus, we need only account for the direction of the cliff to determine the direction of the gradient. As we have argued that we need not worry too much about the magnitudes cancelling, we

need only to solve for where the cliff-edge curve of equation (42) is perpendicular to $\nabla\mathcal{F}_{\text{back}}$ to find the point where the directions cancel and so the approximate saddle-point values for ϕ and $\boldsymbol{\xi}$. Doing so, we arrive at the condition

$$L\left(\frac{l_p^3}{8}+\frac{9}{2}v_p l_p\phi+\left(\frac{l_p^2}{4}+3v_p\phi\right)^{\frac{3}{2}}\right)=V|\psi|\sqrt{\frac{3v_p}{2}}\left(l_p+\sqrt{\frac{l_p^2}{4}+3v_p\phi}\right). \tag{43}$$

Our solution assumes $\boldsymbol{\xi}$ and $\boldsymbol{\psi}$ are antiparallel, as they should be at an extremum of the free energy. Equation (43) constitutes a cubic equation in ϕ

$$\begin{aligned}27\phi^3 v_p^3 L^4 &- \frac{27}{4}\phi^2 v_p^2\left(2l_p^2L^4+14v_p l_p L^2|\psi|^2V^2+3v_p^2|\psi|^4V^4\right)\\&+\frac{9}{16}\phi v_p l_p^2\left(3l_p^2L^4+16v_p l_p L^2|\psi|^2V^2+78v_p^2|\psi|^4V^4\right)\\&-\frac{27}{4}v_p\frac{l_p^4}{16}|\psi|^2V^2\left(2l_pL^2+3v_p|\psi|^2V^2\right)=0.\end{aligned} \tag{44}$$

The resulting (positive real) solution is rather complicated, and we will denote it simply as ϕ_c. Applying ϕ_c to equation (42), we solve for an equivalent $|\boldsymbol{\xi}|_c$, and now expand the free energy of equation (38) in powers of the binormal order parameter magnitude $|\psi|$.

5. Binormal alignment transition

Substituting the optimal solutions for ϕ_c and $|\boldsymbol{\xi}|_c$ (which are too cumbersome to write here explicitly) to the expression for the free energy, equation (38), we expand it in powers of the binormal order parameter magnitude $|\psi|$. The result of this expansion takes the form

$$\beta\mathcal{F}\approx\frac{A}{2}|\psi|+\frac{B}{4}|\psi|^2+\frac{C}{6}|\psi|^3+O(|\psi^4|), \tag{45}$$

where the coefficients are given by

$$A=\frac{V}{18}\left[9+\frac{8\sqrt{3l_p^3}(\sqrt{8}-3)}{\sqrt{2v_p}}\right]\approx V\left(0.50-0.093\sqrt{\frac{l_p^3}{v_p}}\right) \tag{46}$$

$$B=\frac{4V^2}{L}\left[(\sqrt{8}-3)\frac{l_p}{2}+\frac{7\sqrt{3v_p}}{32\sqrt{2l_p}}+\lambda\frac{L}{V}\right]\approx\frac{V^2}{L}\left(-3.43l_p+1.07\sqrt{\frac{v_p}{l_p}}+4\lambda\frac{L}{V}\right) \tag{47}$$

$$C=\frac{6V^3}{L^2}\left[\frac{(6\sqrt{2}-7)\sqrt{v_p l_p}}{2\sqrt{6}}-\frac{5v_p}{256l_p}\right]\approx\frac{V^3}{L^2}\left(1.82\sqrt{v_p l_p}-0.12\frac{v_p}{l_p}\right). \tag{48}$$

The cubic coefficient C is positive for $v_p<240.8l_p^3$. Since we have already calculated that $v_p^*=4l_p^3/9$ for a semi-flexible chain without binormal interactions in section 2, this condition is satisfied automatically for chains with semi-flexible statistics.

One might wonder about the linear coefficient A, which would seem to act like an external field. Since an external field usually induces a non-zero solution for the order parameter at all times, this would seem to rule out any interesting phase behaviour. However, $|\psi|>0$, so we need not consider the 'solution' of the Landau free energy that occurs at $|\psi|<0$ for $A>0$. Since $|\psi|$ is necessarily positive, we can make the substitution $V|\psi|\equiv\eta^2$, where η

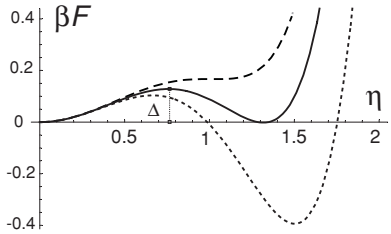

Figure 6. Graph of free energy $\beta\mathcal{F}$ against the dimensionless order parameter η before the transition (dashed line, $B_0 = -2\sqrt{A_0C_0}$), at the transition point (solid line, $B_0 = -2.31\sqrt{A_0C_0}$), and past the transition (dotted line, $B_0 = -2.7\sqrt{A_0C_0}$). We have taken $A_0, C_0 = 1$, and fix $\beta\mathcal{F}_{\eta=0} = 0$ for all plots. Note the presence of the energy barrier Δ separating the coexisting states at the transition.

is a non-dimensional scalar. We so obtain the equivalent Landau free energy expansion in a form more familiar in the theory of phase transformations:

$$\beta\mathcal{F} = \tfrac{1}{2}A_0\eta^2 + \tfrac{1}{4}B_0\eta^4 + \tfrac{1}{6}C_0\eta^6.$$

The Landau coefficients, taken in the limit $v_p^* = 4l_p^3/9$, are given by

$$A_0 \approx 0.36 \qquad B_0 \approx 4[0.093\, l_p/L + \lambda/V] \qquad C_0 \approx 1.16\, l_p^2/L^2.$$

This free energy expansion describes a phase transition from a random-coil state with $|\psi| = 0$ to a binormally aligned state, similar to what the left end of the sketch in figure 4 looks like. The transition is first-order (discontinuous) for $B = -4\sqrt{AC/3}$ if $\{A, C\} > 0$. It has a continuous, second-order nature for $A < 0$. Such transition behaviour is common in, e.g., ferroelectric phase transformations [33]. In terms of the model parameters, we reach the tricritical point of $A = 0$ when $v_p \approx 0.035l_p^3$. Thus, the transition will be second-order for v_p smaller than this value, and first-order for larger v_p. In our case we demand that a polymer chain is equivalent to the classical semi-flexible case in the absence of binormal interaction, that is, we set $v_p = v_p^*$. The resulting value of the Landau coefficient A_0 indicates that our system will always exhibit a discontinuous first-order transition.

In this first-order regime, the transition will occur when the strength of effective binormal interaction $\lambda \approx -0.244l_p(V/L)$, if we continue using the value for compression volume parameter $v_p^* = 4l_p^3/9$ and the resulting Landau coefficients A_0, B_0 and C_0. This prediction rests comfortably with our intuition, as it indicates that the system will undergo any aligning transition at $\lambda \lesssim 0$, and specifically as the interaction strength $|\lambda|$ approaches the value of the chain rigidity, l_p. We illustrate the free energy for this first-order transition in figure 6, graphing it against η above ($B_0 > -4\sqrt{A_0C_0/3}$), at ($B_0 = -4\sqrt{A_0C_0/3}$), and beyond ($B_0 < -4\sqrt{A_0C_0/3}$) the transition point. Past the transition, we see that the system maintains a meta-stable disordered state, which is separated from the ordered ground state of $\psi \sim \lambda$. The two states are held apart by an energetic barrier

$$\Delta = \frac{(B_0^2 - 4A_0C_0)^{\frac{3}{2}}}{12C^2}$$

(in dimensionless units).

This barrier controls the transition rate into the ordered state, which in the first approximation takes the standard Arrhenius form $k = k_0 e^{-\Delta}$, where k is the transition rate and k_0 the àttempt rate' rate in the high-temperature limit.

We note, however, that the binormal alignment transition can only occur if the 'line concentration' ratio of the space bounding the chain to the chain length, V/L, is itself finite. In terms of the Edwards contact interaction, equation (39) indicates that the ratio $L/V = \rho$, while the quadratic term in ρ in equation (25) suggests for $\nu > 0$ the free energy has a minimum at $\rho \to 0$. Thus, no transition can take place in the $\nu > 0$ case. Provided we have Gaussian random-walk statistics in the $L \to \infty$ limit for the ideal chain with no excluded volume interaction at all ($\nu = 0$) and a radius of gyration $R_g \propto L^{1/2}$, we still find that the transition cannot occur, since $V/L \propto L^{1/2}$, appropriately divergent at $L \to \infty$. Ultimately, one requires a chain in a compact folded conformation, such that $R_g^2 \propto L^{\frac{2}{3}}$ for $L \to \infty$. This condition should hold for chains which have undergone collapse to a globular conformation, as should occur when the coefficient ν in equation (17) becomes negative. In our model, ρ is no longer bounded in this case, but higher-order contact terms ($\propto O(\rho^3)$ or higher) will prevent the true concentration from becoming infinite [8, 34]. One can also imagine that even for positive ν, a melt of chains in the interpenetrating regime should satisfy the concentration requirements for a transition to a binormally aligned state [35].

In fact, this coupling of the binormal alignment transition to a collapse transition resolves some potential theoretical difficulties associated with the binormal alignment transition. The persistence length $l_p \equiv \epsilon/(kT)$ and binormal interaction parameter $\lambda \equiv \sigma/(kT)$, both scale as $(kT)^{-1}$ if one assumes that the underlying potential energies ϵ and σ are at best weakly temperature-dependent. Thus, one would not anticipate passing across the transition condition $\lambda \approx -0.244 l_p(V/L)$ as one varies the temperature, as the ratio of λ to l_p should remain constant in the first approximation. Admittedly, changes in ion concentration or other solvent properties might affect the two parameters differently and so change their ratio. Nevertheless, a temperature-induced binormal alignment transition is still possible, when one crosses the critical temperature of a collapse transition. Such a transition to a more compact form will dramatically reduce the (V/L) prefactor in front of l_p, and so bring the chain past the binormal transition point. This is suggestively like the general theoretical understanding of protein folding, in which a generic collapse transition to a 'liquid drop' brings about other orderings within the chain that culminate in a highly structured native state [36].

One might wonder if the binormal interactions we introduce allow for a collapse to a globule in the first place. Admittedly, we do not repeat here the full globular ground-state stability analysis used by Kholodenko, Moore, and others [9, 10] to assess this collapse transition, but we feel such a step is largely unnecessary. Binormal alignment will certainly impact the internal structure of a globule, but most likely not its overall stability, since there is no direct coupling between binormal order ψ and density ρ in the equations that govern the saddle point of ρ. When we do address the collapse, our approximation of ρ as a constant over some volume is essentially that which the ground-state analysis authors make to deal with the complicated nonlinear differential equations that follow from their formalisms.

6. Conclusions

Assuming that the binormally aligned phase we hypothesize exists, one is naturally led to speculate as to what this phase might look like on a mesoscopic level. For a single chain without volume interactions, the ground state would clearly be a flat circle or a circular 'ribbon', with a radius $r_{\mathrm{circ}} \sim (b^2 L v_p/|\lambda|)^{1/3}$, the variable b being the polymer width. This radius is essentially determined by a competition between persistence length (connected to v_p in the above) that will straighten the circle, and the binormal interaction that tightens it. Of course, real polymers with appreciable chain width and steric interactions cannot collapse to

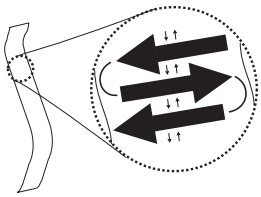

Figure 7. Diagram of proposed anti-parallel beta-sheet structure for amyloid strands typical of insulin and some designed amyloidogenic peptides [42]. Here, the black arrows indicate the 'direction' of the peptide chain (C → N) and small arrows the orientation of hydrogen bonds (O → H).

a flat, completely dense state, but it seems reasonable to claim that the ground state should be a minimal modification of the flat circle: a regular helix. The pitch p between turns of such a helix would be roughly the chain width b, and the radius approximately that given above.

This clearly suggests an analogy to helix-forming peptides in nature. In fact, polypeptides and artificial helicogenic polymers [37–41] possess interactions remarkably similar to the short-range binormal contact interaction presented in this paper. Almost all such systems form associations (hydrogen bonds, aromatic linkages, etc.) that favour chains stacking in the direction perpendicular to their planes of curvature, just as our interaction does. Admittedly, real polymers like polypeptides cannot form helices of arbitrary radius, since hydrogen-bonding sites are not spaced continuously on the chain. As well, we have not yet introduced any terms into the Hamiltonian that would favour a chirally pure helix like α-helices, but the non-zero value of ψ in equation (44) suggests that chiral symmetry can indeed be broken in the binormally aligned state of our model. A right-handed helix of arc length L pointing along the z-axis with a pitch p and a turning rate of w radians per unit arc length s will have a binormal order parameter $\psi_{\rm helix} = \sqrt{1-(pw/(2\pi))^2}L\hat{\boldsymbol{z}}$, which is just the average projection of the binormal on the $\hat{\boldsymbol{z}}$ axis. A left-handed helix will have ψ pointing in the opposite direction. Thus, a totally helical chain consisting of an equal mix of chiralities should have $\psi = 0$, but a non-zero ψ indicates some spontaneous symmetry breaking between handednesses in our system. Chiral symmetry should be preserved in the limit of infinite chain length for polymers with random-walk statistics, where $L/V \propto \lim_{L\to\infty} L^{-1/2} = 0$ as we have noted earlier. Indeed, disorder in the $L \to \infty$ limit is exactly what general Lifson–Roig models predict. Nevertheless, the transition to a binormally aligned state with $\psi \neq 0$ in our model will only occur if the binormal ordering is coupled to a chain globular collapse such that $L/V \to 1$, a collapse step that Lifson–Roig models do not incorporate.

We might also see a binormally aligned phase in a solution of long chains, where one may expect a dense, melt-like phase of directionally aligned chains with aligned binormals. Such systems are known to exist in polypeptides as β-sheet (amyloid) fibrils, where hydrogen bonding plays the role of the binormally aligning interaction. The hydrogen bonds, in turn, tend to line up the peptide 'ribbons' into a sheet, as seen in figure 7. Our analysis significantly strengthens recent suggestions [43, 44] that β-sheet phases arise out of the generic polymer properties of the polypeptide chain. However, our analysis does not rest on simple geometric factors to generate fibril-like structures, but explicitly incorporates the anisotropic bonding of real peptides (already shown to be important in simulation of minimal models of secondary structure) through the binormal contact interactions we describe. One might readily test the peptide-polymer analogy by looking for fibrillar phases in some of the artificial helicogenic polymers discussed above, which we expect will form β-sheet structures when placed in a melt under some conditions. The analogy with amyloid fibrils also suggests some details

about the kinetics of the binormal-alignment transition; experimental peptide results suggest a nucleation-and-growth mechanism in the transition, which may well apply for our model in the first-order transition regime.

Despite the promise of these further directions, we must note some shortcomings of our model. Indeed, a significant fault in our analysis is the fact that our choice of the order parameter $|\psi| = |\int \mathrm{d}s\, \boldsymbol{b}_s \delta[\boldsymbol{R} - \boldsymbol{r}_s]|$ may not capture all of the information about the system's behaviour. After all, the anti-aligning case $\lambda > 0$ could result in a system where the chains' binormal vectors are aligned along a common axis, but have no net binormal orientation, as occurs with chains' tangential vectors in a nematic system. This concern could be redressed by adopting the symmetric part of the binormal orientation tensor $\Psi^{\alpha\beta} = \int \mathrm{d}s\, \boldsymbol{b}_s^\alpha \boldsymbol{b}_s^\beta \delta[\boldsymbol{R} - \boldsymbol{r}(s)]$ as an order parameter as is done in nematic systems, [2] but the quartic dependence of $\Psi^{\alpha\beta}$ on $\boldsymbol{u}(s)$ raises integrability issues which go beyond this paper's level of analysis. Yet despite these difficulties, one can still qualitatively predict some properties of an anti-aligned system. After all, it seems a good heuristic argument that symmetry requires the chain binormals to assume an anti-aligned order for some range of parameters with $\lambda > 0$, much as they possess aligned order for some values of v_p, l_p, etc. for $\lambda < 0$. The structure of an anti-aligned phase may not be much different from that of an aligned phase, save that chains' binormals will point in opposing directions when they intersect. The anti-aligning case with $\lambda > 0$ would not have a helical ground state as the $\lambda < 0$ situation does, but pleated-sheet ground states should be present in both.

In keeping with the issue of modelling an anti-aligned system, one might also object that it would be better to attempt to model a 'binormal nematic' by changing the binormal interaction to $(\boldsymbol{b}_s \cdot \boldsymbol{b}_{s'})^2 \delta[\boldsymbol{r}_s - \boldsymbol{r}_{s'}]$. This would certainly be a better model of interactions between some aromatic rings, which are not as specifically oriented as an O $\rightarrow$ H hydrogen bond. Unfortunately, such a model would encounter the same integrability problem with quartic dependence on $\boldsymbol{u}_s$ as a model with the order parameter $\Psi^{\alpha\beta}$, but such a system would likely be amenable to Monte Carlo analysis.

It is also worth noting that we expect difficulties in applying our theory extremely close to the transition point, as it is only mean-field and neglects fluctuations. The mean-field character of our analysis may also raise troubles with the order of the transition, which mean-field theory does not always predict correctly [33], again as a consequence of neglecting fluctuations. Still, the success of Edwards and Gupta's mean-field theory of nematic polymers at predicting experimental results [2, 3, 45] gives us confidence in general relevance of our model and points the way towards the increased application of analytic methods to complex polymer systems.

Acknowledgments

We thank Sir Sam Edwards and Cait MacPhee for useful discussions and insights that aided the work of this paper. This research has been made possible by a grant from the Gates Cambridge Trust.

References

[1] Flory P J 1984 *Adv. Polymer Sci.* **59** 1
[2] Gupta A M and Edwards S F 1993 *J. Chem. Phys.* **98** 1588
[3] Gupta A M and Edwards S F 1993 *Polymer* **34** 3112
[4] Holyst R and Vilgis T A 1996 *Macromol. Theory Simul.* **5** 573
[5] Warner M W and Terentjev E M 2003 *Liquid Crystal Elastomers* (Oxford: Oxford University Press)

[6] Flory P 1942 *J. Chem. Phys.* **10** 51
[7] Huggins M L 1942 *Ann. NY Acad. Sci.* **43** 1
[8] Edwards S F 1965 *Proc. Phys. Soc.* **85** 613
[9] Moore M A 1977 *J. Phys. A: Math. Gen.* **10** 305
[10] Kholodenko A L and Freed K F 1984 *J. Chem. Phys.* **80** 900
[11] Fixman M 1973 *J. Chem. Phys.* **58** 1559
[12] Yamakawa H 1997 *Helical Wormlike Chains in Polymer Solutions* (Berlin: Springer)
[13] Kratky O and Porod G 1949 *Rec. Trav. Chim.* **68** 1106
[14] B Y Ha and Thirumalai D 1995 *J. Chem. Phys.* **103** 9408
[15] B Y Ha and Thirumalai D 1997 *J. Chem. Phys.* **106** 4243
[16] Whittaker E T 1937 *A Treatise on the Analytical Dynamics of Particles and Rigid Bodies* 4th edn (Cambridge: Cambridge University Press)
[17] Gray A 1998 *Modern Differential Geometry of Curves and Surfaces with Mathematica* 2nd edn (New York: CRC Press)
[18] Teixeira P I C and Terentjev E M 1998 *Eur. Phys. J.* B **3** 237
[19] Muthukumar M and Nickel B G 1984 *J. Chem. Phys.* **80** 5839
[20] Birshtein T M and Pryamitsyn V A 1991 *Macromolecules* **24** 1554
[21] DeGennes P 1972 *Phys. Lett.* A **32** 229
[22] DeGennes P 1979 *Scaling Concepts in Polymer Physics* (Ithaca, NY: Cornell University Press)
[23] Vilgis T A, Johner A and Joanny J F 2000 *Eur. Phys. J.* E **2** 289
[24] Nowak C and Vilgis T A 2004 *Europhys. Lett.* **68** 44
[25] Nowak C, Rostiashvili V G and Vilgis T A 2005 *Macromol. Chem. Phys.* **206** 112
[26] Kemp J P and Chen J Z Y 2001 *Biomacromolecules* **2** 389
[27] Kamien R D 2002 *Rev. Mod. Phys.* **74** 953
[28] Nyrkova I A *et al* 1996 *J. Phys. II* **6** 1411
[29] Nyrkova I A, Semenov A N and Joanny J F 1997 *J. Phys. II* **7** 847
[30] Nyrkova I A, Semenov A N and Joanny J F 1997 *J. Phys. II* **7** 825
[31] Golestanian R and Liverpool T B 2000 *Phys. Rev.* E **62** 5488
[32] Moroz J D and Nelson P 1997 *Proc. Natl. Acad. Sci. USA* **94** 14418
[33] Toledano J-C and Toledano P 1987 *The Landau Theory of Phase Transitions* (Singapore: World Scientific)
[34] Vilgis T A 2000 *Phys. Rep.-Rev. Sec. Phys. Lett.* **336** 167
[35] Doi M and Edwards S F 1986 *The Theory of Polymer Dynamics* (Oxford: Clarendon)
[36] Pande V S, Grosberg A Y and Tanaka T 2000 *Rev. Mod. Phys.* **72** 259
[37] Nelson J C *et al* 1997 *Science* **277** 1793
[38] Rowan A E and Nolte R J M 1998 *Angew. Chem.-Int. Edit.* **37** 63
[39] Kirshenbaum K, Zuckermann R N and Dill K A 1999 *Curr. Opin. Struct. Biol.* **9** 530
[40] Hill D J *et al* 2001 *Chem. Rev.* **101** 3893
[41] Nakano T and Okamoto Y 2001 *Chem. Rev.* **101** 4013
[42] Jaroniec C P *et al* 2004 *Proc. Natl Acad. Sci. USA* **101** 711
[43] Dobson C M 2003 *Nature* **426** 884
[44] Banavar J R *et al* 2004 *Phys. Rev.* E **70** 041905
[45] Podgornik R, Rau D C and Parsegian V A 1994 *Biophys. J.* **66** 962